Published in final edited form as:

AJNR Am J Neuroradiol. 2016 March ; 37(3): 462–467. doi:10.3174/ajnr.A4560.

Magnetic Resonance Elastography Demonstrates Increased Brain Stiffness in Normal Pressure Hydrocephalus

Fattahi N, **Arani A**, **Perry A**, **Meyer F**, **Manduca A**, **Glaser K**, **Senjem ML**, **Ehman RL**, and **Huston J**

Abstract

Introduction—Normal pressure hydrocephalus (NPH) is a reversible neurologic disorder characterized by a triad of cognitive impairment, gait abnormality and urinary incontinence that is commonly treated with ventriculoperitoneal shunt placement. However, there are multiple overlapping symptoms which often make it difficult to differentiate NPH from other types of dementia and improved diagnostic techniques would help patient management. MR elastography (MRE) is a novel diagnostic tool that could potentially identify patients with NPH. The purpose of this study was to assess brain stiffness changes in NPH patients compared with age- and sex-matched cognitively normal individuals.

Methods—MRE was performed on 10 NPH patients and 21 age- and sex-matched volunteers with no known neurologic disorders. Image acquisition was conducted on a 3T MRI scanner. Shear waves with 60Hz vibration frequency were transmitted into the brain by a pillow-like passive driver. A novel postprocessing technique resistant to noise and edge artifacts was implemented to determine regional brain stiffness. The Wilcoxon rank sum test and linear regression were used for statistical analysis.

Results—A significant increase in stiffness was observed in the cerebrum ($p = 0.001$), occipital lobe ($p = 0.0002$), parietal lobe ($p= 0.001$), and the temporal lobe ($p = 0.02$) in the NPH group compared with normal controls. However, no significant difference was noted in other regions of the brain including the frontal lobe ($p = 0.07$), deep gray and white matter ($p = 0.43$), or the cerebellum ($p = 0.20$).

Corresponding Author: John Huston III, MD, Professor of Radiology, Mayo Clinic, Rochester, jhuston@mayo.edu, ph: (507) 284-2804.

DISCLOSURES: Nikoo Fattahi—*RELATED: Grant:* Theodore W. Batterman Family Foundation and R01 grants EB001981 (R.L.E.).* **Armando Manduca**—*UNRELATED: Stock/Stock Options:* Stockholder in Resoundant, which works in the general area of MR elastography. **Kevin Glaser**—*RELATED: Grant:* NIH R01 EB001981*; *UNRELATED: Patents (planned, pending or issued):* MR Elastography*; *Royalties:* Licensing of MR Elastography Intellectual Property; *Stock/Stock Options:* Resoundant, Inc. **Matthew Senjem**—*RELATED: Grant:* NIH.* **Richard Ehman**—*RELATED: Grant:* NIH (EB00181)*; *UNRELATED: Board Membership:* Resoundant, Inc. (CEO, uncompensated); *Grants/Grants Pending:* Resoundant Inc.; *Patents (planned, pending or issued):* RLE and the Mayo Clinic have patents and intellectual property rights related to MRE; *Royalties:* Resoundant, Inc., Comments: Resoundant has licensed MRE technology from Mayo Clinic. Resoundant pays a licensing fee to Mayo Clinic, which is shared in part with RLE and other inventors, pursuant to the Bayh-Dole act; *Stock/Stock Options:* Resoundant Inc*; *OTHER RELATIONSHIPS:* The Mayo Clinic and RLE have intellectual property rights and a financial interest in technologies used in this research. RLE serves and CEO of Resoundant, Inc. This research conducted under oversight and in compliance with Mayo Clinic Conflict of Interest Review Board. **John Huston**—*RELATED: Grant:* NIH (NIH R01 grants EB001981),* Theodore W. Batterman Family Foundation*; *UNRELATED: Patents (planned, pending or issued):* MR Elastography brain patents planned; *Stock/Stock Options:* Resoundant, Inc.
*money paid to institution

Conclusion—This study demonstrates increased brain stiffness in NPH patients compared to age- and sex-matched normal controls which motivates future studies investigating the use of MRE for NPH diagnosis and efficacy of shunt therapy.

Keywords

Normal pressure hydrocephalus (NPH); Magnetic Resonance Elastography (MRE); Brain Stiffness

INTRODUCTION

Normal pressure hydrocephalus (NPH) is a potentially treatable condition characterized by cognitive impairment, gait abnormality and urinary incontinence. A recent large epidemiologic study reported a dramatic increase in the prevalence of NPH after the age of 80 with only a minority of these cases undergoing treatment [1]. With the progressive aging of our population, a continued increase in the prevalence of NPH can be expected in the future.

Multiple overlapping signs and symptoms between different types of cognitive impairment such as NPH, Alzheimer's disease and vascular dementia [2-4] create diagnostic challenges in patients with cognitive impairment. This motivates the development and investigation of novel noninvasive imaging techniques to serve as diagnostic tools for identifying patients with NPH. The reversibility of neurologic symptoms after shunt tube placement supports the theory that deranged cerebrospinal fluid (CSF) circulation could play a role in NPH pathophysiology. Hypothetically, CSF accumulation may lead to local compression on the brain and be the cause of this disorder [4]. Therefore, recent studies have targeted hemodynamic and CSF circulation alterations and are investigating their role in intracranial pressure changes, which may be the cause of neurologic symptoms in NPH [5-7].

Although there is variability in the diagnosis of NPH, a high-volume lumbar tap with improvement of clinical symptoms assessed by video studies obtained before and after the procedure is considered the most sensitive test for NPH at our institution. Several groups have shown that there is a strong correlation between surgical outcomes of shunt placement and patient's response to high-volume lumbar tap [5, 8-13]. However, several factors including time intervals between CSF taps, CSF leaks, and the subjective nature of both the diagnosis and therapeutic response may result in ambiguity in the interpretation of the results. Another disadvantage of a lumbar tap is the invasive nature of the test, with associated potential complications such as headache, infection and CSF leakage [14]. Neuroimaging currently has a prominent role in the diagnosis, assessment of therapy response, and monitoring of disease progression in NPH patients. Disproportionate enlargement of cerebral ventricles, the sylvian fissure and the basal cistern in relation to the degree of cortical atrophy are conventional magnetic resonance imaging (MRI) findings suggestive of NPH [15].

Magnetic resonance elastography (MRE) is an MRI-based technique that noninvasively measures the mechanical properties of tissues *in vivo*. It has been shown that pressure changes that alter tissue elasticity are detectable by MRE [16, 17]. Therefore, the purpose of

this study was to investigate possible brain stiffness change in NPH patients compared with age- and sex-matched normal controls.

METHODS

This study was approved by our institutional review board and all subjects provided informed written consent prior to recruitment and imaging.

Subjects

Ten NPH patients (5 females and 5 males) with a mean age of 71 (range 67-79) were studied. All subjects were diagnosed with NPH based on clinical symptoms and enlarged ventricles out of proportion to the size of the sulci (anatomical MR imaging) and a significant improvement of symptoms following high-volume lumbar tap (Table 1). After performing MRE, all patients underwent CSF shunt surgery and nine out of ten patients experienced a significant improvement in symptoms after the procedure which further supports the NPH diagnosis. Twenty-one healthy cognitively normal individuals without known neurologic disorders, 11 females and 10 males with mean age 74 (67-80), served as the normal control group. The normal control group was obtained from a subset of subjects previously recruited from a longitudinal study of aging and imaged with MRE [18, 19].

MRE

Studies were performed on a 3.0T scanner (GE Healthcare, Milwaukee, WI, USA) using a single-shot, flow-compensated, spin-echo EPI pulse sequence. Shear waves were introduced into the brain from an active driver engine located outside of the scan room through a soft pillow-like passive driver placed under the subject's head within an 8-channel receive-only head coil [20]. The frequency of vibration was 60 Hz and the MRE sequence was performed using the following parameters: TR/TE=3600/62 ms; field of view (FOV)=24 cm; BW= ±250 kHz; 72×72 imaging matrix reconstructed to 80×80; 3x parallel imaging acceleration, frequency encoding in the anterior-posterior direction; 48 contiguous 3-mm-thick axial slices; one 4-G/cm 18.2-ms zeroth- and first-order moment nulled motion-encoding gradient on each side of the refocusing RF pulse synchronized to the motion; motion encoding in the positive and negative x, y and z directions; and 8 phase offsets sampled over one period of the 60 Hz motion (the acquisition time was under 7 minutes). The acquired images had 3-mm isotropic resolution.

Image Processing

We applied a previously published MRE postprocessing pipeline that masks out voxels with significant contributions from cerebral spinal fluid, minimizes partial volume and edge effects, attempts to correct areas of low MR signal-to-noise ratio (SNR) and low wave amplitude, and has previously been shown to have a coefficient of variation of less than 1% for global brain stiffness and less than 2% for the lobes of the brain and the cerebellum [21]. Key features of the processing are: registration of the MRE data to a standard anatomical atlas, applying the vector curl operation on the first temporal harmonic of the acquired displacement field to reduce the effects of longitudinal waves and boundaries; adaptive filters for all derivative calculations to reduce partial volume effects at boundaries; and

careful masking of the results from regional boundaries to minimize edge effects and contamination from CSF. The curl is a mathematical operation on a vector field (in this case, the displacement field with motion in all three directions). It is a combination of derivatives that quantifies rotational deformation (e.g. shear waves), which is the only signal of interest in MRE, but suppresses all compressional deformation (e.g. longitudinal waves). Lastly, An elastogram (map of stiffness, defined as wave speed squared times density) was calculated by applying the direct inversion algorithm to the smoothed curl wave field. Additionally two phase offset images were acquired with zero motion amplitude in order to calculate the signal-to-noise ratio. We calculated the median stiffness of different regions of interest (ROIs) in the brain. Each ROI was generated by applying a warped lobar atlas to a T1 weighted image. ROIs were then registered to the magnitude data obtained from the MRE as described previously [22]. The full post-processing pipeline to produce elastograms was applied separately to each ROI. The ROIs investigated in this study included the cerebrum (whole brain excluding cerebellum), frontal, temporal, parietal, occipital lobes, deep gray matter/white matter (GM/WM) (insula, deep gray nuclei and white matter tracts) and the cerebellum.

Statistical Analysis

In order to compare brain tissue stiffness between NPH patients and normal controls, a Wilcoxon rank sum test was used and a p-value of less than 0.05 was considered statistically significant. A linear regression test was used to determine whether or not sex and age introduced a significant bias in the brain stiffness of the normal control cohort.

Results

The average median stiffness value of the cerebrum among NPH patients was 2.64 +/− 0.1 kPa, which was significantly higher than the stiffness of the cerebrum in normal controls, 2.55 +/−0.1 kPa ($p = 0.001$) (Figure 1). Significant increased stiffness was also observed in the occipital lobe ($p = 0.0002$), the parietal lobe ($p= 0.001$) as well as the temporal lobe ($p = 0.02$) in the NPH group (Figures 2 and 3). However, no significant difference was noted in other regions of the brain including the frontal lobe ($p = 0.07$), deep GM/WM ($p = 0.43$) or the cerebellum ($p = 0.20$) (Table 2). Brain stiffness of the normal control group was fitted to a linear regression model to assess possible confounding factors of age and sex in the specific age range. A trend with age was found as in previous work [19] although in this age range it did not reach statistical significance (p-value 0.1). There was no significant linear relationship between sex and brain stiffness in our normal control group (p-value 0.8).

Discussion

In our study, NPH patients demonstrated a significant increase of stiffness in the cerebrum and in the occipital, parietal, and temporal lobes compared with age- and sex-matched normal controls. Although, there is a significant difference between NPH patients and normal control (Figure 1) there is too much overlap between the groups to be useful on an individual patient basis. Our findings stand in contrast to those of Streitberger et al. [23] who observed a significant decrease in the cerebral stiffness in NPH patients compared to age- and sex-matched normal controls. This discrepancy may be attributed to differences in the acquisition and postprocessing techniques. In our study, we reported on 3-mm isotropic full

volume data sets segmented into anatomical lobes, while Streitberger et al. took three adjacent 6-mm-thick slices and segmented them into global and periventricular regions. A considerable volume of Streitberger's region of interest included the frontal lobes, which in our work showed a trend towards decreased stiffness in NPH patients (although it did not reach significance). Other differences between Streitberger's technique and ours, including differences in scanner hardware; processed data resolutions (1.5×1.5×6 mm vs. 3×3×3 mm); TE (149 ms vs. ~60 ms); number of time points (32 vs. 8); and a processing approach that attempts to minimize CSF contamination and edge effects in this study all could potentially introduce SNR differences and stiffness estimation variations between the two techniques.

The physiology of NPH is dynamic, complex, and not well understood, which makes it difficult to deduce a concrete mechanism behind the brain stiffening observed in this study. NPH generally refers to ventricular enlargement with normal opening pressure on lumbar puncture. However, overnight intermittent elevation of the intracranial pressure has been detected in NPH patients suggesting that increased ICP may play a role in the pathophysiology of NPH [24]. In addition, Alperin et al. reported a linear pressure-volume relationship between volumetric blood flow rate and ICP changes with a consistent elastance index [25]. Based on these findings, ventricular dilatation is thought to occur at the expense of the compressible compartment, as interstitial and intracellular fluids are “squeezed” out of parenchymal pores. Brain tissue compression can cause tissues to move into the nonlinear elastic regime, causing stiffening, which would support our findings. Furthermore, corresponding cellular changes, such as a higher ratio of cytoskeletal matrix to interstitial and intracellular fluid have been reported, as well as a more compressed capillary and venous channel matrix, all of which could contribute to parenchymal stiffening and a loss of compliance[26, 27].

In this study we found a significant increase in stiffness in the occipital, parietal and temporal lobes, while lower elasticity values were measured in the frontal lobe and deep GM/WM areas in NPH patients compared to healthy controls. Although these latter findings did not reach significance, it attracted our attention towards possible underlying changes that may contribute to brain softening. Several imaging and histopathological studies reported brain tissue degeneration beyond the paraventricular area, which was shown to be associated with acute or chronic hydrocephalus [28-30]. Ziegelitz et al. illustrated a significant reduction in cerebral blood flow, not only in the paraventricular area but also in the basal medial frontal cortex and deep grey matter in NPH patients compared to healthy controls. Also, they reported a positive correlation between decreased cerebral blood flow and severity of clinical symptoms [31]. Bugalho et al. suggested that predominant frontal lobe white matter lesions observed by T2-weighted MRI may be a cause of irreversible symptoms in NPH [32]. Therefore, the combination of factors such as reduced blood flow, tissue degeneration, and the development of white matter lesions could result in tissue softening in some regions, which may be overcompensating compressional stiffening effects.

Further evidence of these competing factors can be found in the diffusion-tensor imaging (DTI) literature. DTI studies investigating microstructural changes in NPH have illustrated region-dependent neuronal changes throughout the brain. They have reported that neuronal

integrity changes in the periventricular area, including the corticospinal tract, are consistent with changes secondary to mechanical compression and tend to reverse after shunt treatment. However, neuronal integrity changes in the frontal lobe white matter, corpus callosum and deep grey matter are compatible with degenerative changes, which remain unchanged after treatment [6, 7, 29, 32-34]. Furthermore, previous brain MRE studies on Alzheimer's disease and multiple sclerosis illustrated that decreased brain tissue stiffness is associated with neurodegenerative changes [20, 33, 34]. Similarly, in this study we hypothesize that the decreased stiffness in the frontal lobe and deep GM/WM may be attributed to the underlying neurodegenerative process resulting from NPH or reduced blood flow [13, 24, 35, 36]. Increased pressure in these areas, producing elevated stiffness, due to ventricle enlargement may also contribute to a limited measurable reduction in stiffness. This theory is also compatible with clinical and neuroanatomical studies suggesting that cognitive impairment in NPH corresponds to irreversible changes in the deep GM/WM frontal subcortical areas, which is unlikely to improve after shunt treatment [37, 38]. Also, Freimmann et al. have reported no significant change in stiffness after shunt tube placement in NPH patients [39]. These results motivate future investigation into the relationship between regional brain stiffness and shunt placement outcomes.

Conclusion

Brain MRE of patients with NPH revealed increased brain tissue stiffness in the cerebrum and the occipital, parietal and temporal lobes compared with age- and sex-matched normal controls. Although not significant, decreased stiffness was observed in the frontal lobe and deep GM/WM of NPH patients when compared to healthy controls. This specific pattern of stiffness alteration motivates future studies investigating the role of compressibility and degenerative changes in the development of NPH. In the future, MRE could potentially be implemented as a valuable diagnostic and prognostic tool for NPH and therapy response.

Acknowledgements

This research was supported by Theodore W. Batterman Family Foundation and R01 grants EB001981 (R.L.E.).

References

1. Jaraj D, et al. Prevalence of idiopathic normal-pressure hydrocephalus. Neurology. 2014; 82(16): 1449–54. [PubMed: 24682964]
2. Leinonen V, et al. Cortical brain biopsy in long-term prognostication of 468 patients with possible normal pressure hydrocephalus. Neurodegener Dis. 2012; 10(1-4):166–9. [PubMed: 22343771]
3. Bech-Azeddine R, et al. Idiopathic normal-pressure hydrocephalus: clinical comorbidity correlated with cerebral biopsy findings and outcome of cerebrospinal fluid shunting. J Neurol Neurosurg Psychiatry. 2007; 78(2):157–61. [PubMed: 17012342]
4. Chakravarty A. Unifying concept for Alzheimer's disease, vascular dementia and normal pressure hydrocephalus - a hypothesis. Med Hypotheses. 2004; 63(5):827–33. [PubMed: 15488655]
5. Bateman GA. The pathophysiology of idiopathic normal pressure hydrocephalus: cerebral ischemia or altered venous hemodynamics? AJNR Am J Neuroradiol. 2008; 29(1):198–203. [PubMed: 17925373]
6. Kamiya K, et al. Axon diameter and intra-axonal volume fraction of the corticospinal tract in idiopathic normal pressure hydrocephalus measured by q-space imaging. PLoS One. 2014; 9(8):e103842. [PubMed: 25093733]

7. Klinge PM, et al. Correlates of local cerebral blood flow (CBF) in normal pressure hydrocephalus patients before and after shunting--A retrospective analysis of [(15)O]H(2)O PET CBF studies in 65 patients. Clin Neurol Neurosurg. 2008; 110(4):369–75. [PubMed: 18262344]
8. Wikkelso C, et al. The clinical effect of lumbar puncture in normal pressure hydrocephalus. Journal of neurology, neurosurgery, and psychiatry. 1982; 45(1):64–9.
9. Damasceno BP, et al. The predictive value of cerebrospinal fluid tap-test in normal pressure hydrocephalus. Arquivos de neuro-psiquiatria. 1997; 55(2):179–85. [PubMed: 9629375]
10. Marmarou A, et al. The value of supplemental prognostic tests for the preoperative assessment of idiopathic normal-pressure hydrocephalus. Neurosurgery. 2005; 57(3 Suppl):S17–28. discussion ii-v. [PubMed: 16160426]
11. Calcagni ML, et al. Regional cerebral metabolic rate of glucose evaluation and clinical assessment in patients with idiopathic normal-pressure hydrocephalus before and after ventricular shunt placement: a prospective analysis. Clinical nuclear medicine. 2013; 38(6):426–31. [PubMed: 23640238]
12. Lundin F, et al. Postural function in idiopathic normal pressure hydrocephalus before and after shunt surgery: a controlled study using computerized dynamic posturography (EquiTest). Clinical neurology and neurosurgery. 2013; 115(9):1626–31. [PubMed: 23489444]
13. Lundin F, et al. How active are patients with idiopathic normal pressure hydrocephalus and does activity improve after shunt surgery? A controlled actigraphic study. Clinical neurology and neurosurgery. 2013; 115(2):192–6. [PubMed: 22673042]
14. Kahlon B, Sundbarg G, Rehncrona S. Comparison between the lumbar infusion and CSF tap tests to predict outcome after shunt surgery in suspected normal pressure hydrocephalus. J Neurol Neurosurg Psychiatry. 2002; 73(6):721–6. [PubMed: 12438477]
15. Kitagaki H, et al. CSF spaces in idiopathic normal pressure hydrocephalus: morphology and volumetry. AJNR Am J Neuroradiol. 1998; 19(7):1277–84. [PubMed: 9726467]
16. Hirsch S, et al. Compression-sensitive magnetic resonance elastography. Phys Med Biol. 2013; 58(15):5287–99. [PubMed: 23852144]
17. Mousavi SR, et al. Measurement of in vivo cerebral volumetric strain induced by the Valsalva maneuver. J Biomech. 2014; 47(7):1652–7. [PubMed: 24656483]
18. Roberts RO, et al. The Mayo Clinic Study of Aging: Design and sampling, participation, baseline measures and sample characteristics. Neuroepidemiology. 2008; 30(1):58–69. [PubMed: 18259084]
19. Arani A, et al. Measuring the effects of aging and sex on regional brain stiffness with MR elastography in healthy older adults. Neuroimage. 2015; 111:59–64. [PubMed: 25698157]
20. Murphy MC, et al. Decreased brain stiffness in Alzheimer's disease determined by magnetic resonance elastography. J Magn Reson Imaging. 2011; 34(3):494–8. [PubMed: 21751286]
21. Murphy MC, et al. Measuring the characteristic topography of brain stiffness with magnetic resonance elastography. PLoS One. 2013; 8(12):e81668. [PubMed: 24312570]
22. Jack CR Jr. et al. 11C PiB and structural MRI provide complementary information in imaging of Alzheimer's disease and amnestic mild cognitive impairment. Brain. 2008; 131(Pt 3):665–80. [PubMed: 18263627]
23. Streitberger KJ, et al. In vivo viscoelastic properties of the brain in normal pressure hydrocephalus. NMR in biomedicine. 2011; 24(4):385–92. [PubMed: 20931563]
24. Eide PK, Brean A. Cerebrospinal fluid pulse pressure amplitude during lumbar infusion in idiopathic normal pressure hydrocephalus can predict response to shunting. Cerebrospinal Fluid Res. 2010; 7:5. [PubMed: 20205911]
25. Alperin NJ, et al. MR-Intracranial pressure (ICP): a method to measure intracranial elastance and pressure noninvasively by means of MR imaging: baboon and human study. Radiology. 2000; 217(3):877–85. [PubMed: 11110957]
26. Sklar FH, et al. Brain elasticity changes with ventriculomegaly. J Neurosurg. 1980; 53(2):173–9. [PubMed: 6893601]
27. Levine DN. The pathogenesis of normal pressure hydrocephalus: a theoretical analysis. Bull Math Biol. 1999; 61(5):875–916. [PubMed: 17886748]

28. Del Bigio MR, Cardoso ER, Halliday WC. Neuropathological changes in chronic adult hydrocephalus: cortical biopsies and autopsy findings. Can J Neurol Sci. 1997; 24(2):121–6. [PubMed: 9164688]
29. Tarnaris A, et al. Cognitive, biochemical, and imaging profile of patients suffering from idiopathic normal pressure hydrocephalus. Alzheimers Dement. 2011; 7(5):501–8. [PubMed: 21757406]
30. Assaf Y, et al. Diffusion tensor imaging in hydrocephalus: initial experience. AJNR Am J Neuroradiol. 2006; 27(8):1717–24. [PubMed: 16971621]
31. Ziegelitz D, et al. Cerebral perfusion measured by dynamic susceptibility contrast MRI is reduced in patients with idiopathic normal pressure hydrocephalus. J Magn Reson Imaging. 2014; 39(6): 1533–42. [PubMed: 24006249]
32. Bugalho P, Alves L. Normal-pressure hydrocephalus: white matter lesions correlate negatively with gait improvement after lumbar puncture. Clin Neurol Neurosurg. 2007; 109(9):774–8. [PubMed: 17768003]
33. Murphy MC, et al. Magnetic resonance elastography of the brain in a mouse model of Alzheimer's disease: initial results. Magn Reson Imaging. 2012; 30(4):535–9. [PubMed: 22326238]
34. Streitberger KJ, et al. Brain viscoelasticity alteration in chronic-progressive multiple sclerosis. PLoS One. 2012; 7(1):e29888. [PubMed: 22276134]
35. Qvarlander S, et al. Pulsatility in CSF dynamics: pathophysiology of idiopathic normal pressure hydrocephalus. J Neurol Neurosurg Psychiatry. 2013; 84(7):735–41. [PubMed: 23408066]
36. Hamlat A, et al. Theoretical considerations on the pathophysiology of normal pressure hydrocephalus (NPH) and NPH-related dementia. Med Hypotheses. 2006; 67(1):115–23. [PubMed: 16530979]
37. Poca MA, et al. Good outcome in patients with normal-pressure hydrocephalus and factors indicating poor prognosis. J Neurosurg. 2005; 103(3):455–63. [PubMed: 16235677]
38. Kazui H. [Cognitive impairment in patients with idiopathic normal pressure hydrocephalus]. Brain Nerve. 2008; 60(3):225–31. [PubMed: 18402069]
39. Freimann FB, et al. Alteration of brain viscoelasticity after shunt treatment in normal pressure hydrocephalus. Neuroradiology. 2012; 54(3):189–96. [PubMed: 21538046]

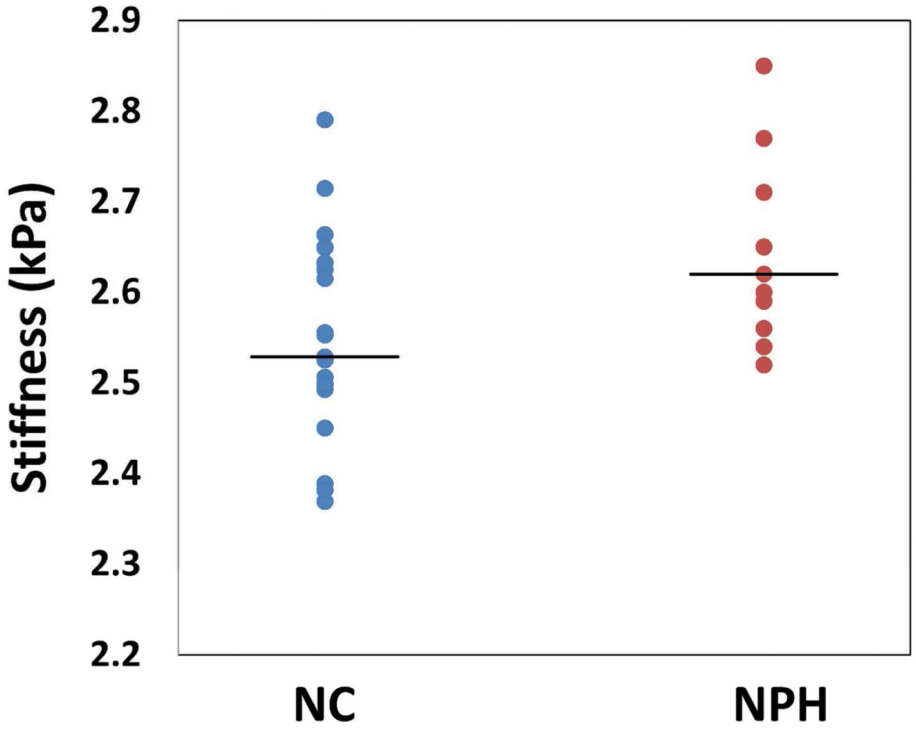

Figure 1.

Summary of cerebral stiffness for the normal control (NC) and normal pressure hydrocephalus (NPH) patients. Lines represent the median stiffness for each group and the circles represent the cerebral median stiffness for each individual patient.

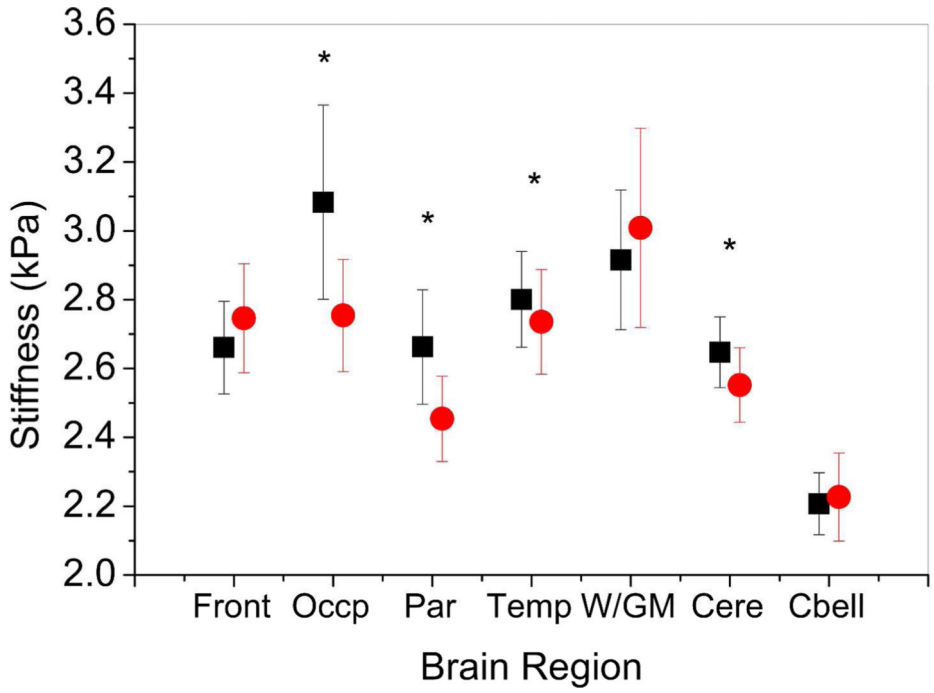

Figure 2.

Mean of the median stiffness and standard deviation of brain regions in normal pressure hydrocephalus patients (black squares) and normal controls (red circles). Asterisks (*) indicate regions of significant stiffness difference between the NPH group and the normal controls. Frontal lobe (Front), Occipital lobe (Occp), Parietal lobe (Par), Temporal lobe (Temp), Deep white/gray matter (W/GM), Cerebrum (Cere), Cerebellum (Cbell).

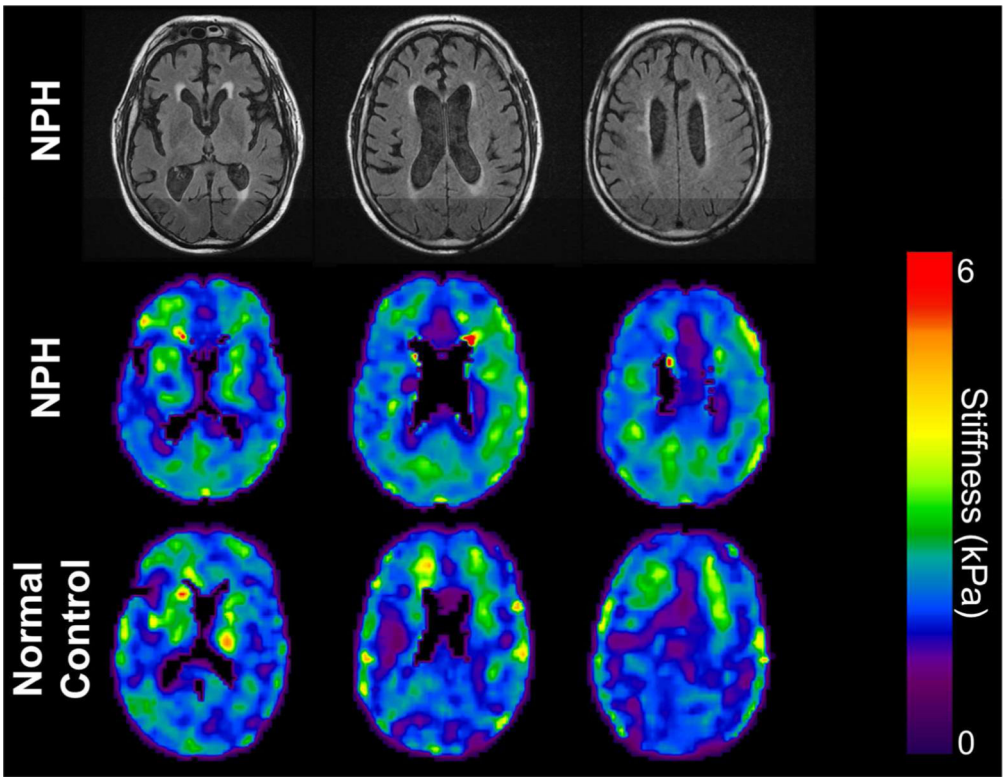

Figure 3.
MRE image comparison of NPH and NC patients. T2 FLAIR images (1st row) and MRE images (2nd row) of a 67 year old male with NPH. MRE of an age- and sex-matched normal control (3rd row). MRE shows increased stiffness in the NPH patient compared with the normal control, especially in the parietal and occipital regions.

Table 1

patient's distribution based on clinical manifestations and clinical response to treatment.

Clinical Symptoms	100% gait disturbance 80% cognitive problems 50% urinary incontinence
High volume CSF tap	100% Significant improvement
Response to shunt treatment	90% Significant improvement 10% No improvement

Table 2

MRE stiffness results.

	Normal Control Brain Stiffness (kPa)	NPH Brain Stiffness (kPa)	p-value
Frontal lobe	2.75 ± 0.16	2.66 ± 0.13	0.07
Occipital lobe	2.75 ± 0.16	3.08 ± 0.28	0.0002
Parietal lobe	2.45 ± 0.12	2.66 ± 0.17	0.001
Temporal lobe	2.73 ± 0.15	2.80 ± 0.14	0.02
Deep GM/WM	3.01 ± 0.29	2.91 ± 0.20	0.43
Cerebrum	2.55 ± 0.11	2.65 ± 0.10	0.001
Cerebellum	2.23 ± 0.13	2.21 ± 0.09	0.20